# Hybrid observer for improved transient performance of a marine vessel in dynamic positioning ⋆

**Astrid H. Brodtkorb** * **Svenn A. Værnø** * **Andrew R. Teel** **
**Asgeir J. Sørensen** * **Roger Skjetne** *

* *Centre for Autonomous Marine Operations (NTNU AMOS), Department of Marine Technology, Norwegian University of Science and Technology (NTNU), Otto Nielsens vei 10, 7491 Trondheim, Norway (e-mails: astrid.h.brodtkorb@ntnu.no, svenn.are.varno@ntnu.no, asgeir.sorensen@ntnu.no, roger.skjetne@ntnu.no).*
** *Department of Electrical and Computational Engineering, University of California Santa Barbara, CA USA (e-mail: teel@ece.ucsb.edu)*

**Abstract:** Dynamic positioning (DP) systems are used on marine vessels for automatic station keeping and tracking operations solely by use of thrusters. Observers are key components of DP systems, and two main types are proposed in this paper. The model-based type is used in steady state conditions since it is especially good at filtering out first order wave induced motions and predicting states in the case of signal loss, and the signal-based type typically has superior performance during transients. In this paper a hybrid observer including a signal-based part and a model-based part with a performance monitoring function is proposed. The observer part that provides the best estimate of the vessel position and heading is used in closed-loop control, thereby allowing for improved transient response while maintaining good steady-state performance. The contributions of this paper include the design of a hybrid signal-based and model-based observer with performance monitoring, stability analysis of the vessel with hybrid estimates in output feedback control, and simulations of a platform supply vessel during a setpoint and heading change.

*Keywords:* Dynamic positioning, observers, hybrid systems, output feedback control

## 1. INTRODUCTION

Marine operations are moving further from shore and into harsher environments, and with it requirements for the DP vessel's operational window, safety functions and energy-efficiency become stricter. Vessels that are doing operations with longer duration experience changing sea states with varying wind and wave directions, with suboptimal heading at times. Large forces and moments act on the vessel, making quick and precise control essential, especially when operating close to other offshore infrastructures.

There are many unknown factors at sea that may cause transients in the vessel response depending on the type of operations: wave trains, ice loads, mooring line break, etc. However, many transients are triggered by the operator, which makes them easier to account for with proactive control strategies, e.g. heading and setpoint changes, pipelay operations, well intervention operations, the lowering of a jack-up vessel from jacked-up to floating, etc. In this work the transient response of a DP vessel is improved by combining two observers.

⋆ This work was supported by the Research Council of Norway through the Centres of Excellence funding scheme, project number 23254 - AMOS, and in part by NSF grant number ECCS-1508757 and AFOSR grant number FA9550-15-1-0155.

The model-based observer, like the Extended Kalman filter (Tannuri and Morishita, 2006), (Hassani et al., 2013), or the nonlinear passive observer (Fossen and Strand, 1999), are commonly used in DP systems. The model-based observer uses noisy position and heading angle measurements to estimate the low frequency position, heading, and velocity of the vessel. A key feature of this observer type is the wave filter, which eliminates the wave frequency vessel motion from the output feedback control law. This reduces the wear and tear on the machinery as well as reducing the energy consumption.

The signal-based observer, also referred to as a kinematic, or sensor-based observer, is based on the kinematic equations, see for instance Mahony et al. (2008), Hua (2010), Grip et al. (2012), and Bryne et al. (2015). It is especially well suited during transients, as it uses linear acceleration measurements to predict velocity and position. In this implementation no wave filter was included in this observer, but it is ongoing work by Bryne et al. (2016). As a result this observer estimates the total vessel motion, including low frequency and wave frequency motion. When inserted into the control law it gives an oscillatory thrust command.

Earlier hybrid control theory has been applied to dynamic positioning in a changing sea state, see Nguyen et al.

(2007) and Brodtkorb et al. (2014), and for changing operational modes (Nguyen et al., 2008). These all consist of a bank of controllers and observers with a supervisory mechanism that monitors performance and chooses the best controller/observer pair. Dwell-time and hysteresis switching were applied to avoid chattering. In this paper we apply an output feedback DP controller, using analysis from Loria et al. (2000). Related to this, Prieur and Teel (2011) looks at output feedback control using a hybrid controller with a nonlinear globally stabilizing part, and a linear locally stabilizing part.

The main contributions of this paper includes the design, analysis, and simulation of a hybrid observer with a model-based part and a signal-based part for improving the transient vessel response in an uncertain marine environment. A performance monitoring function keeps track of the mean estimation error over a time period for the observers, and the estimates from the better-performing observer are used in closed-loop output feedback control using a nonlinear proportional, integral, derivative (nPID) controller. Hysteresis is applied in order to limit the number of jumps for the system, and this is important for the stability of the system.

The organization of the paper is as follows: In Section 2 typical instrumentation for DP vessels is discussed, and two mathematical models of marine DP vessels are presented. A model-based and a signal-based observer are introduced in Section 3, and Section 4 presents the output feedback control algorithm. The hybrid signal-based and model-based observer in closed loop control is modeled in Section 5, and stability is discussed in Section 6. Simulation results for a platform supply vessel doing a setpoint change are presented and discussed in Section 7. Section 8 concludes the paper.

## 2. MARINE VESSEL MODELING AND DYNAMIC POSITIONING

Two reference frames are used in this paper: the North-East-Down (NED) reference frame which is a local Earth-fixed frame, and the body frame, which is body-fixed.

### *2.1 Instrumentation*

DP vessels have statutory class requirements on the onboard instrumentation, and system redundancy. Vessels have positioning systems, e.g. GNSS, acoustics, or laser, a compass measuring heading angle, and an inertial measurement unit (IMU) that combines gyroscopes for measuring angular rates and accelerometers for measuring linear acceleration. The measurements are taken at different sampling rates ranging from 0.1-2 Hz for acoustics, 0.5-4 Hz for GNSS position measurements, to 100-200 Hz for IMU angular velocity and acceleration measurements. The measurements are in this paper assumed to be of the form

$$p^n = [N, E]^\top \tag{1a}$$
$$\psi_c = \psi \tag{1b}$$
$$\omega^b_{imu} = \omega^b + b_g \tag{1c}$$
$$f^b_{imu} = R(\Theta)(\dot{v}^n - g^n), \tag{1d}$$

where the measurements in the NED frame have superscript $n$, and measurements in the body frame have superscript $b$. $p^n \in \mathbb{R}^2$ is the measured position in north and east. A heave measurement may also be obtained through GNSS, but it is typically of low quality and is not used here. $\psi_c \in \mathbb{R}$ is measured heading angle ($\psi$ is used in the remainder of the paper), $\omega^b_{imu} \in \mathbb{R}^3$ is measured angular rate $\omega^b$, $f^b_{imu} \in \mathbb{R}^3$ is measured linear acceleration, $\Theta = [\phi,\ \theta,\ \psi]^\top \in \mathbb{R}^3$ is the orientation in roll, pitch and yaw, $R(\Theta) \in \mathbb{R}^{3\times 3}$ is the rotation matrix about the $z, y, x$ axes, $g^n \in \mathbb{R}^3$ is acceleration due to gravity, and $b_g \in \mathbb{R}$ is the gyro bias. Measurement noise is disregarded in the stability analysis, but inserted in simulations.

### *2.2 Marine vessel modeling*

Two models of the same system are presented.

*Control plant model* The control plant model for a vessel is a simplification of the real vessel dynamics. It is different for the various vessel types, operational and environmental conditions, and the design problem under consideration (e.g. observer design or feedback control design); see Fossen (2011) or Sørensen (2013). A surface vessel in DP with starboard/port symmetry, $M = M^\top$, has largest motions in the horizontal plane (surge, sway, and yaw), so the heave, roll, and pitch dynamics are neglected. The control plant model in this case is:

$$\dot{\xi} = A_w \xi + E_w w_w, \tag{2a}$$
$$\dot{\eta} = R(\psi)\nu, \tag{2b}$$
$$\dot{b} = -T_b^{-1} b + E_w w_b \tag{2c}$$
$$M\dot{\nu} = -D\nu + R^\top(\psi) b + u, \tag{2d}$$
$$y = \eta + W\xi + v_y; \tag{2e}$$

where the states of the system include the 3 DOF North, East position and heading $\eta := [N, E, \psi]^\top$ and body-fixed velocity $\nu$ in surge, sway and yaw. In normal operational conditions we want to control only the low frequency part of the vessel motion, and the wave filter in (2a) allows us to separate the motion into a wave frequency part, and a low frequency part. The wave filter has a state $\xi \in \mathbb{R}^6$ and system matrix $A_w \in \mathbb{R}^{6\times 6}$ that contains the peak wave frequency and damping. It is driven by zero mean white noise $w_w$. (2b-d) are the low frequency dynamics of the vessel. (2b) is the 3 DOF kinematics that transforms velocity from the body to the NED frame; $R(\psi)$ is the rotation matrix about the $z$-axis,

$$R(\psi) = \begin{bmatrix} \cos(\psi) & -\sin(\psi) & 0 \\ \sin(\psi) & \cos(\psi) & 0 \\ 0 & 0 & 1 \end{bmatrix}. \tag{3}$$

The wave frequency part of the heading angle, $\psi_w$, is assumed to be small, $R(\psi+\psi_w) \approx R(\psi)$. (2c) is a bias force model with state $b \in \mathbb{R}^3$, accounting for *slowly-varying* environmental disturbances from mean wind, current, and second-order wave loads and unmodeled vessel dynamics. $T_b$ is the Markov time constant, and $w_b$ zero mean white noise. Note that the bias force model does not capture rapidly varying disturbances. In (2d) $M \in \mathbb{R}^{3\times 3}$ is the inertia matrix including added mass for asymptotic values of wave frequency equal to zero, $D \in \mathbb{R}^{3\times 3}$ is the linear damping coefficient matrix, and $u \in \mathbb{R}^3$ is the control input. (2e) is the measurement $y = [(p^n)^\top\ \psi]^\top \in \mathbb{R}^3$ of

position and heading including low frequency motion $\eta$, wave frequency motion $W\xi$ with $W = [0_{3\times3},\ I_{3\times3}]$, and measurement noise $v_y$.

*Kinematic model* The kinematic model is based on fundamental principles of inertia, relating position, velocity and acceleration of the vessel in 6 DOF. It represents the same vessel as in (2), but now the acceleration and angular velocities are inputs as well as the position and heading. The dynamics are split into a translational part and an angular part. The translational part is written as

$$\dot{p}^n = v^n \tag{4a}$$

$$\dot{v}^n = R(\Theta) f^b_{imu} + g^n. \tag{4b}$$

$p^n$ is the north, east and down (heave) position and $v^n$ is the NED velocity. The acceleration measurements from the IMU are rotated directly to the NED frame. The orientation of the vessel is $\Theta$ in roll, pitch, and yaw angles, and $R(\Theta)$ is the 6 DOF rotation matrix about the $z, y, x$-axes. Gravity is also acting on the vessel. The attitude part is written as

$$\dot{\Theta} = T(\Theta)\omega^b \tag{5}$$

with the velocity transformation matrix $T(\Theta)$ and angular rate $\omega^b$.

Relating the two models, we have that

$$\eta = [p^n(1),\ p^n(2),\ \psi]^\top,$$
$$\nu = R(\psi)^\top [v^n(1),\ v^n(2),\ \omega^b(3)]^\top. \tag{6}$$

## 3. OBSERVERS USED IN DYNAMIC POSITIONING

The two observers are briefly presented in this section. The reader is referred to Fossen and Strand (1999), Fossen (2011) for details on the model-based observer, and to Grip et al. (2012), Grip et al. (2013), Bryne et al. (2014), and Bryne et al. (2015) for details on the signal-based observer.

### *3.1 Model-based observer*

We have chosen to work with the nonlinear passive observer (Fossen and Strand, 1999) since it is an intuitive observer to tune, and it has global stability results. This is based on the control plant model (2) taking in position and heading measurements, and commanded thrust $u$ from the controller (see Section 4). It is a 3 DOF observer, and the algorithm can be written as

$$\dot{\hat{\xi}} = A_\omega \hat{\xi} + K_{1,\omega}\tilde{y} \tag{7a}$$

$$\dot{\hat{\eta}} = R(\psi)\hat{\nu} + K_2\tilde{y} \tag{7b}$$

$$\dot{\hat{b}} = T_b^{-1}\hat{b} + K_3\tilde{y} \tag{7c}$$

$$M\dot{\hat{\nu}} = -D\hat{\nu} + R^\top(\psi)\hat{b} + u + R^\top(\psi)K_4\tilde{y} \tag{7d}$$

$$\hat{y} = \hat{\eta} + C_\omega\hat{\xi}, \tag{7e}$$

where $\hat{\xi}, \hat{\eta}, \hat{v}, \hat{b} \in \mathbb{R}^3$ are the estimates of the states in (2), $\tilde{y} = y - \hat{y}$ is the measurement estimation error and $K_{1,\omega} \in \mathbb{R}^{6\times3}_{>0}, K_2, K_3, K_4 \in \mathbb{R}^{3\times3}_{>0}$ are observer gains chosen to satisfy the Kalman-Yakubovich-Popov (KYP) lemma (Khalil, 2002). The wave filter contains estimates of the peak wave frequency and damping in $A_\omega \in \mathbb{R}^{6\times6}$, and $C_\omega = W$ from (2). The key feature in this observer is the wave filter. This means that the wave frequency motion $W\xi$ is separated from the low frequency motion $\eta$, and the output from this observer is the *low frequency motion* estimate of the vessel: $\hat{\eta}_1 := \hat{\eta}$ and $\hat{\nu}_1 := \hat{\nu}$.

Define the estimation errors as $\tilde{(\cdot)}:=(\cdot)$ - $\hat{(\cdot)}$, and collect them in the state $x_1 := [\tilde{\nu}^\top,\ \tilde{\eta}^\top,\ \tilde{\xi}^\top,\ \tilde{b}^\top]^\top$. The error dynamics of (2) and the model-based observer (7) is written compactly as

$$\dot{x}_1 = F_1(x_1, p^n, \psi). \tag{8}$$

### *3.2 Signal-based observer*

The signal-based observer is a 6 DOF observer, and is based on the kinematic relations (4) and (5). The attitude is represented using quaternions, $q$.

*Attitude observer* Write the attitude observer dynamics as

$$\dot{\hat{q}} = T(\hat{q})(\omega^b_{imu} - \hat{b}_g + \hat{\sigma}) \tag{9a}$$

$$\dot{\hat{b}}_g = Proj(\hat{b}_g, -k_I\hat{\sigma}), \tag{9b}$$

with the correction term

$$\hat{\sigma} = k_1 c^b \times R(\hat{q})^\top c^n + k_2 f^b_{imu} \times R(\hat{q})^\top \hat{f}^n \tag{10}$$

where $\hat{q}$ is the attitude estimate, $T(\hat{q})$ is the velocity transformation matrix, $\hat{b}_g$ is the gyro bias estimate, and a bias compensated angular rate estimate is provided as well $\hat{\omega}^b$. The projection function used is found in (Grip et al., 2012, Appendix). The symbol $\times$ represents the cross product, $c^b = [\cos(\psi),\ -\sin(\psi),\ 0]^\top$, $\psi$ is measured by the compass, and $c^n = [1,\ 0,\ 0]^\top$ is a reference vector. $f^b_{imu}$ is the measured acceleration and $\hat{f}^n$ is the estimated acceleration in NED. Choose the gains $k_1 \geq k_P,\ k_2 \geq k_P$, with $k_P > 0$ sufficiently large.

*Translational Observer* The translational observer is based on (4). The equations are taken from Bryne et al. (2015), as we use a virtual vertical reference in heave in stead of the low quality GNSS measurement. The algorithm is

$$\dot{\hat{p}}^n_I = \hat{p}^n_z + k_{pipi}\tilde{p}_I \tag{11a}$$

$$\dot{\hat{p}}^n = \hat{v}^n + \theta^2 \begin{bmatrix} 0_{2\times1} & K_{pp} \\ k_{ppi} & 0_{1\times2} \end{bmatrix} \begin{bmatrix} \tilde{p}_I \\ \tilde{p} \end{bmatrix} \tag{11b}$$

$$\dot{\hat{v}}^n = \hat{f}^n + g^n + \theta^3 \begin{bmatrix} 0_{2\times1} & K_{vp} \\ k_{vpi} & 0_{1\times2} \end{bmatrix} \begin{bmatrix} \tilde{p}_I \\ \tilde{p} \end{bmatrix} \tag{11c}$$

$$\dot{\xi}_f = -R(\hat{q})S(\hat{\sigma})f^b_{imu} + \theta^4 \begin{bmatrix} 0_{2\times1} & K_{\xi p} \\ k_{\xi pi} & 0_{1\times2} \end{bmatrix} \begin{bmatrix} \tilde{p}_I \\ \tilde{p} \end{bmatrix} \tag{11d}$$

$$\hat{f}^n = R(\hat{q})f^b_{imu} + \xi_f. \tag{11e}$$

The driving errors are defined as: $\tilde{p} = p^n - \hat{p}^n \in \mathbb{R}^2, \tilde{p}_I = p_I - \hat{p}_I = 0 - \hat{p}_I \in \mathbb{R}$. $R(\hat{q})$ is the rotation matrix in roll, pitch, and yaw represented with quaternion estimates from (9). $\xi_f$ is a correction term on the acceleration estimate. $K_{pp}, K_{vp}, K_{\xi p} \in \mathbb{R}^{2\times2}_{>0}$, and $k_{pipi}, k_{ppi}, k_{vpi}, k_{\xi pi} \in \mathbb{R}_{>0}$. $\theta \geq 1$ is a high gain. The equation (11a) includes only the virtual heave part of the position estimate, i.e. it is scalar.

The estimation error state can be written compactly as $x_2 := [\tilde{q}^\top, \tilde{b}_g^\top, \tilde{p}_I, \tilde{p}^\top, \tilde{v}^\top, \tilde{f}^\top]^\top$, with estimation errors defined as before, $\tilde{(\cdot)}:=(\cdot)$ - $\hat{(\cdot)}$. The error dynamics can be written compactly as

$$\dot{x}_2 = F_2(x_2, p^n, \psi, \omega^b_{imu}, f^b_{imu}). \tag{12}$$

The signal-based estimation error dynamics (12) has the origin uniformly locally exponentially stable (ULES) with almost global attractivity (Grip et al. (2012) and Bryne et al. (2015)). The attractivity is almost global but not global; hence, the convergence rate from points near the boundary of the basin of attraction, particularly those corresponding to yaw estimation error equal to 180 degrees, is slow.

The output from the signal-based observer is transformed so it has the same form as the output from the model-based observer using (6)

$$\hat{\eta}_2 := [\hat{p}^n(1),\ \hat{p}^n(2),\ \hat{\psi}_2]^\top$$
$$\hat{\nu}_2 := R(\hat{\psi}_2)^\top [v^n(1),\ v^n(2),\ \hat{\omega}^b(3)]^\top \tag{13}$$

where $\hat{\psi}_2$ is the heading angle estimate we get when converting from quaternions $\hat{q}$ to Euler angles, and the velocity output is transformed from the NED frame to the body frame. Because this observer relies on acceleration measurements and does not include a bias force estimation model, it reacts fast and accurately to transients. The downside to this is that the estimates are not wave filtered, so $\hat{\eta}_2$ and $\hat{\nu}_2$ will cause an oscillatory control input.

## 4. CONTROLLER

The control objective is to control the vessel to the desired time-varying setpoint $\eta_d(t)$ with the desired velocity trajectory $\nu_d(t)$:

$$\lim_{t\to\infty} \eta(t) - \eta_d(t) = 0$$
$$\lim_{t\to\infty} \nu(t) - \nu_d(t) = 0.$$

We write the tracking error dynamics as $x_0 := [\nu - \nu_d,\ \eta - \eta_d,\ \zeta - K_i^{-1} b]$, with the integral state in the controller $\zeta$ defined below.

The control objective is achieved by combining feedforward of the desired trajectory and output feedback using a nonlinear proportional, integral, derivative (nPID) algorithm. The algorithm is

$$\dot{\zeta} = (\hat{\eta}_s - \eta_d) \tag{14a}$$
$$u = -K_p R^\top(\psi)(\hat{\eta}_s - \eta_d) - K_d(\hat{\nu}_s - \nu_d) \tag{14b}$$
$$- K_i R^\top(\psi)\zeta + M\dot{\nu}_d + D\nu_d. \tag{14c}$$

$u \in \mathbb{R}^3$ is the commanded thrust, $K_p, K_d, K_i \in \mathbb{R}^{3\times 3}$ are the proportional, derivative and integral gains, and $\hat{\eta}_s$ and $\hat{\nu}_s$ are the estimates from the model-based observer when $s = 1$, and from the signal-based observer when $s = 2$. $\zeta$ compensates for the unknown bias force in (2d), which is commonly assumed constant for control design. The integral action error is $\zeta - K_i^{-1} b$. $K_i$ should be picked so it can commute with the rotation matrix, i.e. $K_i R(\psi) = R(\psi) K_i$. The last two terms in (14b) are feedforward terms of the desired acceleration times inertia and desired velocity times damping.

Loria et al. (2000) showed that the feedback control law (14) using model-based estimates renders the closed-loop vessel and output feedback controller UGAS.

Following a similar approach for the other observer renders the closed-loop vessel and output feedback controller using signal-based estimates uniformly locally asymptotically stable (ULAS). We conclude local because the desired behavior of the observer error dynamics (12) is predicated on the derivative of the tracking error, $\dot{x}_0$, being bounded. It is not clear whether the region of attraction for the origin of the signal-based output feedback controller and vessel is almost global. The simulations in Section 7 indicate that the basin of attraction when the signal-based estimates are used in feedback is fairly large, but further research on this problem is required to make rigorous statements about the basin of attraction of the origin for (12), (14), (4) and (5).

## 5. HYBRID SIGNAL-BASED AND MODEL-BASED OBSERVER IN CLOSED-LOOP CONTROL

The observers flow in parallel in the hybrid observer design, and the position and velocity in surge, sway, and yaw from the observer that performs best is used in output feedback with (14). The estimation errors are monitored, and switching is limited by hysteresis.

### *5.1 Plant, controller, and observer*

The flow dynamics of the hybrid system constitutes the marine vessel, controller, and observer dynamics is

$$\dot{\eta} = R(\psi)\nu, \tag{15a}$$
$$M\dot{\nu} = -D_L\nu + R^\top(\psi)b + u \tag{15b}$$
$$\dot{\zeta} = \hat{\eta}_s - \eta_d \tag{15c}$$
$$u = -R^\top(\psi)K_p(\hat{\eta}_s - \eta_d) - K_d(\hat{\nu}_s - \nu_d)$$
$$- R^\top(\psi)K_i\zeta + M\dot{\nu}_d + D\nu_d \tag{15d}$$
$$\dot{x}_1 = F_1(x_1, p^n, \psi) \tag{15e}$$
$$\dot{x}_2 = F_2(x_2, p^n, \psi, \omega^b_{imu}, f^b_{imu}) \tag{15f}$$
$$\dot{s} = 0, \tag{15g}$$

with $\eta, \nu, \hat{\eta}_s, \hat{\nu}_s \in \mathbb{R}^3$. (15a-b) are the vessel dynamics, (15c-d) is the control algorithm with output feedback and reference feedforward, (15e) is the model-based observer (7), and (15f) is the signal-based observer from (9) and (11). $s \in \{1, 2\}$ is a logic variable that indicates if the model-based or signal-based estimates are used in closed-loop control. $s = 1$ is model-based and $s = 2$ is the signal-based estimates, as decided by the performance monitoring and switching logic.

### *5.2 Performance monitoring and switching logic*

The performance monitoring function computes the estimation errors of the two observers in position and heading over a time period to make sure the system does not switch unnecessarily often. In order to make a fair comparison, the total (low frequency and wave frequency) estimates are compared with the measured position and heading where north and east positions are measured in meters and heading in degrees. The model-based estimate, including wave frequency components, is $\hat{y}_1 := \hat{y}$ from (7), and the signal-based position and heading estimates are $\hat{y}_2 := \hat{\eta}_2$.

We sample $y$, $\hat{y}_1$, and $\hat{y}_2$ every $T > 0$ seconds and $N \in \mathbb{Z}_{\geq 1}$ consecutive measurements are stored in the state of three different shift registers with states $\chi_k \in \mathbb{R}^{3N}$, $k = \{0, 1, 2\}$. $\chi_{k,i} \in \mathbb{R}^3$, $i \in \{1, \ldots, N\}$ are the stored measurements and estimates. The state component $\chi_{k,1}$ contains the most recent samples, and $\chi_{k,N}$ contains the least recent samples; see (17a-f).

Let $\ell \in \mathbb{R}$ be a counter that triggers a performance check of the observer. This happens every $LT$ seconds where $L \in \mathbb{Z}_{\geq 1}$. Let us define the *shift register mean value* for the measurements: $\bar{\chi}_0 := \frac{1}{N}\sum_{i=1}^{N} \chi_{0,i}$, model-based: $\bar{\chi}_1 := \frac{1}{N}\sum_{i=1}^{N} \chi_{1,i}$, and signal-based: $\bar{\chi}_2 := \frac{1}{N}\sum_{i=1}^{N} \chi_{2,i}$. We switch to the other observer if it performs better than the one currently in feedback with a hysteresis margin of $\varepsilon > 0$; see (17g-i).

The jumps for these variables are allowed when

$$(x_0, x_1, x_2, \chi_k, \tau, \ell, s) \in D \tag{16}$$

$$D := \mathbb{R}^9 \times \mathbb{R}^{15} \times \mathbb{R}^{16} \times \mathbb{R}^{3Nk} \times \{T\} \times \{0, \ldots, L\} \times \{1, 2\}$$

$x_0$ is the tracking error defined in Section 4. The jumps satisfy

$$\chi_{0,1}^{+} = y \tag{17a}$$

$$\chi_{1,1}^{+} = \hat{y}_1 \tag{17b}$$

$$\chi_{2,1}^{+} = \hat{y}_2 \tag{17c}$$

$$\chi_{k,2}^{+} = \chi_{k,1}, \quad k = \{0, 1, 2\} \tag{17d}$$

$$\vdots \tag{17e}$$

$$\chi_{k,N}^{+} = \chi_{k,N-1}, \ k = \{0, 1, 2\} \tag{17f}$$

$$\tau^{+} = 0 \tag{17g}$$

$$\ell^{+} = \begin{cases} \ell + 1 & \ell \in \{0, \ldots, L-1\} \\ 0 & \ell = L \end{cases} \tag{17h}$$

$$s^{+} \in \begin{cases} s & \ell \in \{0, \ldots, L-1\} \\ 3 - s & \ell = L, \ |\bar{\chi}_0 - \bar{\chi}_{3-s}| \leq |\bar{\chi}_0 - \bar{\chi}_s| - \varepsilon \\ s & \ell = L, \ |\bar{\chi}_0 - \bar{\chi}_{3-s}| \geq |\bar{\chi}_0 - \bar{\chi}_s| - \varepsilon. \end{cases} \tag{17i}$$

All the states introduced in this section remain constant during flows, except for $\tau$ that satisfies $\dot{\tau} = 1$. Flows are allowed when

$$(x_0, x_1, x_2, \chi_k, \tau, \ell, s) \in C \tag{18}$$

$$C := \mathbb{R}^9 \times \mathbb{R}^{15} \times \mathbb{R}^{16} \times \mathbb{R}^{3Nk} \times [0, \ T] \times \{0, \ldots, L\} \times \{1, 2\}.$$

## 6. STABILITY

The stability results used to analyze the set are based on invariance and uniform convergence according to Proposition 7.5 of Goebel et al. (2012). Consider the set

$$\mathcal{A} := \{0\} \times \{0\} \times \{0\} \times \Psi \times [0, \ T] \times \{0, \ldots, L\} \times \{1, 2\}, \tag{19}$$

with $\Psi := \{\chi_{0,ss}\} \times \{\chi_{1,ss}\} \times \{\chi_{2,ss}\}$ and $\chi_{k,ss}$, $k = \{0, 1, 2\}$ are the steady-state values of the shift register with saved measurements and estimates of the total vessel motion. The set $\mathcal{A}$ is compact because its components are closed and bounded sets.

*Theorem 1.* The set $\mathcal{A}$ defined in (19) is uniformly locally asymptotically stable (ULAS) for the hybrid system defined in (15)-(18).

*Proof:* The set $\mathcal{A}$ is:

(i) strongly forward invariant. If the solution starts inside the set $\mathcal{A}$, the observer in closed loop, regardless of which, will keep the solution within $\mathcal{A}$ during flows. During jumps the solution still remains in $\mathcal{A}$ since jumping from the set of values $\mathcal{A} \cap D$, will yield a solution that still is in $\mathcal{A}$.

(ii) uniformly attractive from a neighborhood of itself. Since each observer is converging, at least locally, it follows from the switching condition in (17i) that the number of switches will be uniformly bounded, at least from initial conditions sufficiently close to the set $\mathcal{A}$, and that the last switching time can also be uniformly bounded. That is there exists a $T$ such that

$$|\bar{\chi}_0(t) - \bar{\chi}_1(t)| + |\bar{\chi}_0(t) - \bar{\chi}_2(t)| \leq \varepsilon \quad \forall t \geq T,$$

and there will be no more switching. Then, because of uniform attractivity in the absence of switching, we also have uniform attractivity with the switching. □

## 7. SIMULATION RESULTS AND DISCUSSION

Simulations are done in Matlab/Simulink with a platform supply vessel in a marine environment with waves, wind and current. The high fidelity simulation model is based on the MSS GNC toolbox (Fossen and Perez, 2010) with realistic measurement noise and sample time. The sea state is very rough with significant wave height 4 meters, peak frequency 0.6 rad/s taken from the JONSWAP [1] spectrum, with mean incident wave heading 150° in the North-East frame (Price and Bishop, 1974). The current speed is 0.5 m/s with direction 180°, and the wind speed and direction are taken as expectation values based on the wave parameters.

The case simulated is a setpoint change where the vessel moves 20 meters North and East, and changes heading from $\psi = 0°$ to $\psi = -90°$. The change happens at 2500 seconds so the observer parts have ample time to converge to steady state first. Figure 1 shows the estimation error for the signal-based and model-based observer parts after the initialization phase. The switching variable $s$ indicates which observer estimates are used in closed loop.

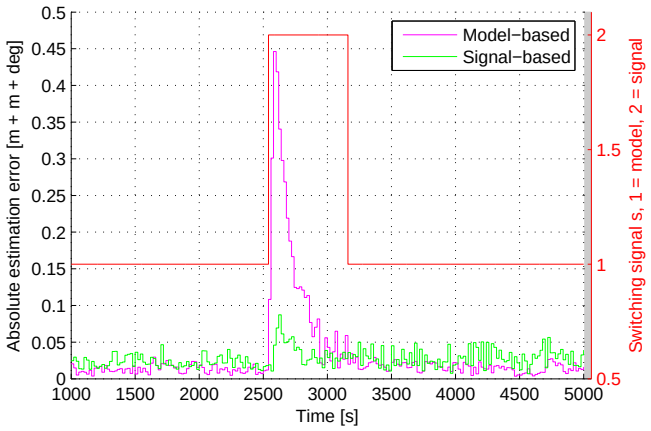


Fig. 1. Estimation error for the signal-based and model-based parts. The estimates used in closed-loop $s$ is indicated, with axis to the right.

At initialization the model-based observer is chosen in feedback, as it takes time for the gyro bias estimate $\hat{b}_g$ in the signal-based observer to converge. The bias force estimate $\hat{b}$ in the model-based observer converges after about 500 seconds. When the vessel changes heading,

[1] Joint North Sea Wave Project.

the forces on the hull due to current, wind and waves changes rapidly. This induces a transient in the model-based part since the bias force estimate takes time to converge to the new value. 40 seconds after the vessel starts the setpoint change, the signal-based observer performs better and is used in feedback. 700 seconds later the model-based bias force estimate $\hat{b}$ has converged to the new value and is used in feedback once more. While performing better during the setpoint change, the signal-based part has higher estimation error during steady state, as seen clearly in the figure. The simulation results indicate that the basin of attraction for the signal-based estimates in output feedback control is fairly large, since it includes points from where we end up switching.

The vessel response is more oscillatory when the signal-based observer is used in closed-loop. This is because the signal-based observer does not include a wave filter and has oscillatory estimates. It therefore induces some wave frequency motion on the system through the control law, approximately $\pm 1$ meter. This motion is insignificant compared with the motion due to the 4 meter waves, however, the vessel uses more energy and in a real system the wear and tear on the machinery would be increased.

## 8. CONCLUSION

The hybrid observer with a signal-based and a model-based part was shown to have good performance in simulations of a DP vessel in a rough sea state. The observer used in output feedback with a nonlinear PID tracking controller, was shown uniformly locally asymptotically stable.

## REFERENCES


Brodtkorb, A.H., Sørensen, A.J., and Teel, A.R. (2014). Increasing the operation window of dynamic positioned vessels using the concept of hybrid control. *ASME 2014 33rd International Conference on Ocean, Offshore and Arctic Engineering Volume 1A: Offshore Technology San Francisco, California, USA, June 813, 2014*.

Bryne, T.H., Fossen, T.I., and Johansen, T.A. (2014). Nonlinear observer with time-varying gains for inertial navigation aided by satellite reference systems in dynamic positioning. *2014 22nd Mediterranean Conference on Control and Automation, MED 2014*, 1353–1360.

Bryne, T.H., Fossen, T.I., and Johansen, T.A. (2015). A virtual vertical reference concept for GNSS/INS applications at the sea surface. *10th Conference on Maneouvring and Control of Marine Craft, MCMC August 24-26 2015 Copenhagen, Denmark*.

Bryne, T.H., Fossen, T.I., and Johansen, T.A. (2016). Design of inertial navigation systems for marine craft with adaptive wave filtering by triple-redundant sensor packages. *To appear in: International Journal of Adaptive Control and Signal Processing*.

Fossen, T.I. (2011). *Handbook of Marine Craft Hydrodyamics and Motion Control*. Wiley.

Fossen, T.I. and Perez, T. (2010). Marine systems simulator, viewed 27.01.2016. URL `http://www.marinecontrol.org`.

Fossen, T.I. and Strand, J.P. (1999). Passive nonlinear observer design for ships using lyapunov methods: full-scale experiments with a supply vessel. *Automatica*, 35(1), 3 – 16.

Goebel, R., Sanfelice, R.G., and Teel, A.R. (2012). *Hybrid Dynamical Systems, Modelling, Stability and Robustness*. Princeton University Press.

Grip, H.F., Fossen, T.I., Johansen, T.A., and Saberi, A. (2013). Nonlinear observer for gnss-aided inertial navigation with quaternion-based attitude estimation. *Proceedings of the American Control Conference*, 272–279.

Grip, H., Fossen, T., Johansen, T., and Saberi, A. (2012). Attitude estimation using biased gyro and vector measurements with time-varying reference vectors. *IEEE Transactions on Automatic Control*, 57(5), 1332–1338. doi:10.1109/TAC.2011.2173415.

Hassani, V., Sørensen, A.J., and Pascoal, A.M. (2013). A novel methodology for robust dynamic positioning of marine vessels: Theory and experiments. *Proceedings of the American Control Conference*, 560–565.

Hua, M.D. (2010). Attitude estimation for accelerated vehicles using GPS/INS measurements. *Control Engineering Practice*, 18(7), 723 – 732. Special Issue on Aerial Robotics.

Khalil, H. (2002). *Nonlinear Systems, Second Edition*. Prentice Hall,.

Loria, A., Fossen, T.I., and Panteley, E. (2000). A separation principle for dynamic positioning of ships: Theoretical and experimental results. *IEEE Transactions on Control Systems Technology*, 8(2), 332–343. doi: 10.1109/87.826804.

Mahony, R., Hamel, T., and Pflimlin, J.M. (2008). Nonlinear complementary filters on the special orthogonal group. *IEEE Transactions on Automatic Control*, 53(5), 1203–1218.

Nguyen, T.D., Sørensen, A.J., and Quek, S.T. (2008). Multi-operational controller structure for station keeping and transit operations of marine vessels. *IEEE Transactions on Control Systems Technology*, 16(3), 491–498.

Nguyen, T.D., Sørensen, A.J., and Tong Quek, S.T. (2007). Design of hybrid controller for dynamic positioning from calm to extreme sea conditions. *Automatica*, 43(5), 768–785.

Price, W.G. and Bishop, R.E.D. (1974). *Probalistic Theory of Ships*. Chapman and Hall, London.

Prieur, C. and Teel, A. (2011). Uniting local and global output feedback controllers. *IEEE Transactions on Automatic Control*, 56(7), 1636–1649. doi: 10.1109/TAC.2010.2091436.

Sørensen, A.J. (2013). *Marine Control Systems, Propulsion and Motion Control of Ships and Ocean structures, Lecture Notes*. Department of Marine Technology, NTNU.

Tannuri, E.A. and Morishita, H.M. (2006). Experimental and numerical evaluation of a typical dynamic positioning system. *Applied Ocean Research*, 28(2), 133–146.